NONPARAMETRIC JOINT SHAPE AND FEATURE PRIORS FOR SEGMENTATION OF DENDRITIC SPINES

Ertunc Erdil[⋆1] *Lavdie Rada*[2] *A. Ozgur Argunsah*[3] *Inbal Israely*[3] *Devrim Unay*[4] *Tolga Tasdizen*[5] *Mujdat Cetin*[1]

[1] Faculty of Engineering and Natural Sciences, Sabanci University, Tuzla, Istanbul, Turkey
[⋆]ertuncerdil@sabanciuniv.edu
[2]Faculty of Engineering and Natural Sciences, Bahcesehir University, Besiktas, Istanbul, Turkey
[3] Champalimaud Neuroscience Programme, Champalimaud Centre for the Unknown, Lisbon, Portugal
[4] Department of Electrical and Electronics Engineering, Izmir University of Economics, Balcova, Izmir, Turkey
[5]Department of Electrical and Computer Engineering, University of Utah, Salt Lake City, UT, USA

ABSTRACT

Multimodal shape density estimation is a challenging task in many biomedical image segmentation problems. Existing techniques in the literature estimate the underlying shape distribution by extending Parzen density estimator to the space of shapes. Such density estimates are only expressed in terms of distances between shapes which may not be sufficient for ensuring accurate segmentation when the observed intensities provide very little information about the object boundaries. In such scenarios, employing additional shape-dependent discriminative features as priors and exploiting both shape and feature priors can aid to the segmentation process. In this paper, we propose a segmentation algorithm that uses nonparametric joint shape and feature priors using Parzen density estimator. The joint prior density estimate is expressed in terms of distances between shapes and distances between features. We incorporate the learned joint shape and feature prior distribution into a maximum *a posteriori* estimation framework for segmentation. The resulting optimization problem is solved using active contours. We present experimental results on dendritic spine segmentation in 2-photon microscopy images which involve a multimodal shape density.

***Index Terms*—** Nonparametric joint shape and feature priors, Parzen density estimator, multimodal shape density, dendritic spine segmentation

1. INTRODUCTION

Segmentation of images having limited and low quality data is a challenging problem and requires prior information about the shape to be segmented for an acceptable solution. For example, given a training set of prostate shapes, prostates in a magnetic resonance image whose boundaries are mostly invisible can be segmented by exploiting prior shape information obtained from the training set. The problem becomes more complex when the training set of shapes involves examples from multiple classes (e.g. due to various forms of pathology) leading to a multimodal shape density. We consider the cases where the prior shape density is multimodal and complex.

An example of such a multimodal shape density is dendritic spines of pyramidal neurons. Dendritic spines are the post-synaptic partners of a synapse. It has been shown that structure of a spine is highly correlated with its function [1, 2]. Spines have two major components, head and neck [3]. Spine head size is correlated with the number of conductive channels it constitutes, hence an important determinant of current goes through it. And spine neck has shown to be compartmentalizing electrical and chemical interaction between spine head and dendrite [4]. Furthermore, spine head shape and neck length as well as neck width change through either regular plasticity mechanisms or pathological conditions [2, 3]. Studying such structure requires accurate segmentation of spines, whose shapes belong to one of several classes. We test the performance of our technique on dendritic spine segmentation problem which involves a multimodal and complex shape density.

Early work on shape-based segmentation that uses level set representation of the shape captures shape variability by applying principal component analysis (PCA) to the space of training shapes [5]. These methods are only capable of handling unimodal, Gaussian-like, shape densities. Kim et al. [6] and Cremers et al. [7] propose a nonparametric framework for handling multimodal shape densities. They estimate underlying shape density by extending Parzen density estimator to the space of training shapes. Then, the learned shape prior distribution is incorporated into a maximum *a posteriori* (MAP) estimation framework for segmentation. The resulting optimization problem is solved by applying gradient descent to the energy functional containing data fidelity and shape prior terms. Data fidelity term plays the role of finding the apparent part of the object to be segmented. Then, shape prior term is added to data fidelity term and the curve is updated with the weighted average of the shapes in the training set and data force. Weights are determined based on distances between the evolving curve and training shapes. Therefore, these approaches possess shortcomings when the curve found by data term is closer to training shapes from a wrong class based on a distance metric.

In this paper, we focus on segmentation problems in which shape distributions are multimodal and complex, but just the shape prior information is not sufficient for effective segmentation. Therefore, unlike the state-of-the-art methods that express the nonparametric shape density based on only pure shape distances, we exploit learned intensity-based or geometric features extracted from specific parts of scene relative to the object of interest as priors. We add discriminative features to the kernel density estimation process and perform segmentation accordingly. In particular, we consider distances between features together with the shape distances using a higher dimensional kernel for computing weight of each shape in the training set. This improves the separability of classes in a higher dimen-

This work has been supported by the Scientific and Technological Research Council of Turkey (TUBITAK) under Grant 113E603.

sional space by using extra information about the features relative to the object of interest.

Our contribution in this paper is a segmentation algorithm that performs segmentation by exploiting nonparametric joint shape and feature priors. To the best of our knowledge, nonparametric joint shape and feature priors have not been proposed for image segmentation. By estimating a more discriminative prior density, our algorithm is able to drive the curve toward the more probable class. Moreover, shape densities in subclasses whose properties can only be expressed with additional shape features, can be captured using our approach. Our approach could also be viewed as a particular way to extend active shape and appearance [8] type models to the nonparametric setting. We present experimental results on dendritic spine segmentation in 2-photon microscopy images. We compare our method with the approach of Kim et al. [6] to show the better accuracy and performance of our approach in segmentation. We also provide comparisons with the joint classification and segmentation approach of Erdil et al. [9].

2. JOINT SHAPE AND FEATURE PRIORS FOR IMAGE SEGMENTATION

In this section, we derive the mathematical formulation of our image segmentation approach that uses nonparametric joint shape and feature priors.

Given a set of intensity images with segmented shape boundaries, we learn prior densities for shapes and features, and then use them in the process of segmenting a new test image. Let us assume that we have n training shapes $\mathbf{C} = \{C_1, C_2, \ldots, C_n\}$ and corresponding set of feature vectors $\mathbf{f} = \{f_1, f_2, \ldots, f_n\}$ extracted from intensity images. Then, the posterior probability of C and f is written using Bayes' rule as

$$p(C, f|data) = \frac{p(data|C, f)p(C, f)}{p(data)} \tag{1}$$

where,

$$p(data|C, f) = \frac{p(f|data, C)p(data|C)}{p(f|C)}. \tag{2}$$

Plugging in Equation (2) into (1) yields

$$p(C, f|data) \propto p(f|data, C)p(data|C)p(C) \tag{3}$$

and $p(C)$ can be written as

$$p(C) = \int p(C, f)\, \mathrm{d}f. \tag{4}$$

Then, Equation (3) becomes

$$p(C, f|data) \propto p(data|C) \int p(f|data, C)p(C, f)\, \mathrm{d}f. \tag{5}$$

Now, let $\hat{f}(data, C_{t=t'})$ be a feature vector extracted from data when the state of curve at time t'. From this point on, one can proceed with various assumptions on the probability densities involved. In our case, we learn $p(C, f)$ nonparametrically from the training data. Also, we use the data term proposed in [9] for dendritic spine segmentation as explained in Section 3. For feature extraction, we assume that features can be extracted perfectly based on the data as well as information about the boundary when it reaches a reasonable state (we will specify what that means in the context of spine segmentation). This leads to the degenerate density:

$$p(f|data, C) = \delta(f - \hat{f}(data, C_{t=t'})) \tag{6}$$

where, $\delta(.)$ is the Dirac delta function. Then, Equation (5) becomes

$$p(C, \hat{f}|data) \propto p(data|C)p(C, \hat{f}). \tag{7}$$

By simply taking the negative logarithm of Equation (7), we can define the following energy function to be minimized

$$E(C, \hat{f}) = -\log p(data|C) - \log p(C, \hat{f}) \tag{8}$$

where,

$$p_{C,\hat{f}}(C, \hat{f}) = \frac{1}{n} \sum_{i=1}^{n} k(d(C, C_i), d(\hat{f}, f_i), \sigma_C, \sigma_f). \tag{9}$$

Note that our density estimation involves training samples from all shape classes involved. Given this framework, one could also estimate class conditional joint shape and feature density by limiting the density estimation to training samples from one class only. In Equations (9), $d(.,.)$ is a distance metric and $k(.,., \sigma_C, \sigma_f)$ is a 2D Gaussian kernel with kernel sizes σ_C and σ_f. Note that, the composite of the 2D kernel and the distance metrics plays the role of an infinite dimensional kernel. A variety of distance metrics can be used in Equations (9). In our experiments, we use the template distance metric for shape distance and L_2 distance metric, $d_{L_2}(.,.)$, for feature distance.

Partial derivative of the energy function given in Equation (8) with respect to C is given as follows:

$$\frac{\partial \log p_{C,\hat{f}}(C, \hat{f})}{\partial C} = \frac{1}{p_{C,\hat{f}}(C, \hat{f})} \frac{1}{{\sigma_C}^2} \frac{1}{n} \cdot \sum_{i=1}^{n} k(d_T(\phi_C, \phi_{C_i}), d_{L_2}(\hat{f}, f_i), \sigma_C, \sigma_f) d_T(\phi_C, \phi_{C_i})(1 - 2H(\phi_{C_i}))\vec{N} \tag{10}$$

where, $H(.)$ is the Heaviside function. Updating the level set representation of the curve, ϕ_C with the negative partial derivative of $E(C, f)$ with respect to C, evolves the curve toward the most probable shape.

3. DENDRITIC SPINE SEGMENTATION IN 2-PHOTON MICROSCOPY IMAGES

In the literature, spines are generally grouped into four classes: mushroom, stubby, thin, and filopodia. We consider two major classes: spines that have a neck (mushroom) and those that do not (stubby) (see Figure 1 for examples from both classes). Spine head part is generally bright and common for all spines in both spine classes. Therefore, it can be segmented in most cases using only a data term [9]. However, prior knowledge is needed for the segmentation of the neck part in mushroom spines. Shape-based methods generally segment the apparent part of the object using only data term. Then, the shape prior term is turned on in the energy functional, and both the data and the shape forces are applied in the remaining segmentation process. In the dendritic spine segmentation problem, since the part found by the data term is the spine head which is common for all spines regardless of their classes, the evolving curve is generally more similar to the shapes in the stubby class based on shape distances. This is because of the effect of the additional neck part in increasing distances to mushroom spines. Therefore, the method of Kim et al. [6] is more likely to evolve the shape toward stubby class regardless of the class of the spine to be segmented. To overcome this limitation, [9] proposed a method for joint classification and segmentation of dendritic spines. First,

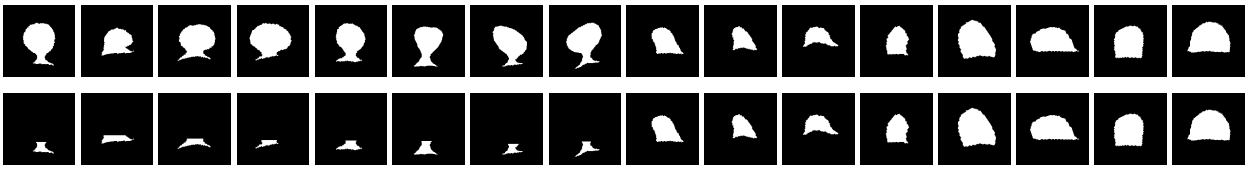

Fig. 1. First row: aligned training set consisting of mushroom and stubby spines for ***Experiment 1***. Note that first 8 spines from left to right are mushroom, the remaining are stubby. Second row: training set of neck shapes and stubby spines for ***Experiment 2***.

the spine head is segmented using a data driven energy functional designed by adding some bias terms to piecewise-constant version of Mumford-Shah functional [12, 10]. After segmentation of the spine head, appearance features are extracted around the spine head and used with a Support Vector Machine classifier. If the spine is classified as stubby, spine head segmentation is returned as the final segmentation. If the spine is classified as mushroom, the approach in [6] is applied with only mushroom examples in the training set. Erdil et al. [9] consider the spine head segmentation as sufficient enough and do not change it during the evolution with shape term. Therefore, training set of mushroom spines is constructed by adding the spine head segmentation on top of a given training set of neck shapes as shown in the second row of Figure 1. Although, [9] presents promising results on dendritic spine segmentation, making a hard decision about the shape class can lead to obtain erroneous segmentations.

We apply our algorithm to dendritic spine segmentation in 2-photon microscopy images. We segment the spine head using the data fidelity term proposed in [9]. Here, spine head segmentation corresponds to the curve $C_{t=t'}$ in Equation (6). Then, we extract both intensity-based (appearance) and geometric features relative to the object of interest. Intensity-based features are obtained by summing up the intensities in a small rectangular region below the spine head horizontally and vertically, and finding intensity histogram in this region [9]. Spine neck length is an important geometric feature for identifying class of a spine. We find this geometric feature by measuring the distance between spine head and dendrite portion in the region of interest [13]. Our training set of shapes consists of spine necks and stubby spines as shown in the second row of Figure 1. Training set of mushroom spines are obtained by adding spine head segmentation on top of spine necks in the training set. Therefore, spine head segmentation will not change during the evolution with shape priors together with the data term. Finally, we keep evolving the curve with the gradient of the energy functional given in Equation (8) until convergence to obtain final spine segmentation.

4. EXPERIMENTAL RESULTS

We perform two different types of experiments to evaluate the performance of our approach. In both type of experiments, we perform segmentations on 24 mushroom and 10 stubby spines, none of which are included in the training set. We evaluate the accuracy of the segmentations by comparing the segmentation results with the ground truths delineated by a domain expert using Dice score [14]. Note that, Dice score takes the highest value of 1 when the perfect match with the ground truth is achieved.

Experiment 1 is performed in order to demonstrate the advantages of our approach over the approach in [6] on evolving the curve toward the shape in the correct class. In this experiment, we construct a training set of shapes involving both mushroom and stubby examples as shown in the first row of Figure 1. We use the geometric feature, neck length [13], that we mentioned in the previous section as discriminative feature in this experiment.

In the left part of Table 1, we present Dice score results together with the likelihood ratios of final segmentation, $\hat{C}$, being in the mushroom class $\big(p_m(\hat{C},\hat{f})$ for the proposed method, $p_m(\hat{C})$ for [6]$\big)$ with respect to the probability of being in stubby class $\big(p_s(\hat{C},\hat{f})$ for proposed method, $p_s(\hat{C})$ for [6]$\big)$[1]. Note that the likelihood ratios, $\frac{p_m(C,f)}{p_s(C,f)}$ and $\frac{p_m(C)}{p_s(C)}$, above 1 for mushroom spines (Spine 1 - 24) and below 1 for stubby spines (Spine 25 - 34) demonstrate that the curve has been driven to the correct class. Such results are shown by bold in the related parts of Table 1. The results show that our method drives the curve toward the correct class for all spines whereas Kim et al. [6] drives toward stubby class for all spines except Spine 4. In Spine 4, the data term captures some part from the neck, hence, the curve become closer to the mushroom spines and [6] can produce a curve from correct class. According to the results, we can conclude that our approach performs better than [6] in terms of evolving curve toward correct class by estimating a more discriminative prior density. Moreover, according to Dice score results, our approach produces better segmentations than [6] on average of 34 spines with this setting of the training set.

In ***Experiment 2***, we use our approach for the dendritic spine segmentation problem as explained in Section 3. In this experiment, we compare the segmentation performance of our approach with [6] and [9]. For all the methods in comparisons, we use the training set shown in the second row of Figure 1 and obtain the training set of mushroom spines by adding spine head segmentation on top of spine necks in the training set. This setting of the training set leads better spine segmentation results as suggested by Erdil et al. [9].

We evaluate the performance of our approach using intensity-based (appearance) and geometric features that we mention in the previous section as priors. We use intensity-based feature vectors by concatenating them into a single feature vector. One can consider using these feature vectors separately by adding extra dimension(s) to the kernel in Equation (9) and changing gradients accordingly.

Constructing training set of mushroom shapes using the spine head segmentation increases the similarity between the evolving curve and the mushroom shapes in the training set compared to the setting of the training set in ***Experiment 1***. Therefore, the method in [6] performs better than ***Experiment 1*** in terms of evolving curve toward a correct class. In ***Experiment 2***, proposed method with both appearance and geometric shape features and [6] produces segmentations from the correct class in all test images. We provide Dice score results on 34 test spine images in the rigth part of Table 1. According to the results, best results are obtained by the proposed method with geometric shape priors on average. Our

[1]Note that $p_m(\hat{C},\hat{f})$ and $p_s(\hat{C},\hat{f})$ can be computed by using only mushroom and only stubby training shapes respectively in Equation (9). Similarly, $p_m(\hat{C})$ and $p_s(\hat{C})$ can be computed by using prior shape density proposed in [6] and using only training shapes from corresponding class.

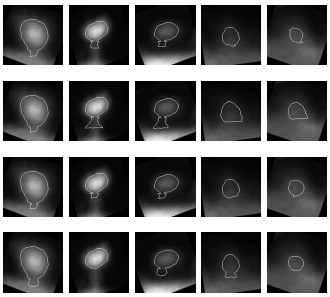

Fig. 2. Visual results obtained in experiment 2 for spines 1, 3, 11, 25, and 26. First row: proposed method with appearance feature, second row: proposed method with geometric feature, third row: Kim et al. fourth row: Erdil et al.

	Experiment 1				***Experiment 2***			
	Proposed Method with Geometric Feature		**Kim et al.** [6]		**Proposed Method with Appearance Feature**	**Proposed Method with Geometric Feature**	**Kim et al.** [6]	**Erdil et al.** [9]
	Dice	$\frac{p_{in}(C_i,f_i)}{p_{ex}(C_i,f_i)}$	**Dice**	$\frac{p_{in}(C_i,f_i)}{p_{ex}(C_i,f_i)}$	**Dice**			
Spine 1	0.759	**1.764**	0.710	0.885	0.875	0.878	0.876	0.869
Spine 2	0.778	**3.657**	0.736	0.821	0.795	0.790	0.792	0.813
Spine 3	0.807	**381.160**	0.724	0.856	0.767	0.787	0.750	0.772
Spine 4	0.728	**4410278.801**	0.677	**1.030**	0.681	0.704	0.657	0.616
Spine 5	0.670	**896.867**	0.685	0.900	0.772	0.738	0.769	0.740
Spine 6	0.762	**2.398**	0.697	0.861	0.750	0.746	0.736	0.748
Spine 7	0.644	**76585655.727**	0.675	0.637	0.662	0.686	0.670	0.675
Spine 8	0.755	**1.443**	0.720	0.955	0.890	0.893	0.889	0.876
Spine 9	0.757	**2.466**	0.713	0.933	0.869	0.870	0.861	0.848
Spine 10	0.829	**2.998**	0.761	0.805	0.856	0.855	0.855	0.851
Spine 11	0.799	**147019.913**	0.763	0.829	0.699	0.767	0.695	0.718
Spine 12	0.839	**12662.596**	0.779	0.837	0.742	0.777	0.737	0.754
Spine 13	0.818	**12.217**	0.822	0.793	0.885	0.894	0.889	0.889
Spine 14	0.641	**54.154**	0.629	0.759	0.882	0.877	0.876	0.895
Spine 15	0.866	**1.132**	0.853	0.768	0.882	0.884	0.882	0.908
Spine 16	0.841	**1.351**	0.814	0.798	0.845	0.859	0.832	0.849
Spine 17	0.828	**2.783**	0.842	0.826	0.784	0.813	0.670	0.801
Spine 18	0.779	**3.244**	0.790	0.781	0.774	0.757	0.756	0.745
Spine 19	0.864	**1.263**	0.828	0.840	0.842	0.826	0.822	0.840
Spine 20	0.836	**1.678**	0.846	0.783	0.908	0.901	0.911	0.884
Spine 21	0.699	**1.683**	0.679	0.994	0.761	0.747	0.769	0.756
Spine 22	0.766	**38.337**	0.719	0.900	0.713	0.673	0.700	0.706
Spine 23	0.762	**7385.921**	0.696	0.941	0.612	0.677	0.614	0.633
Spine 24	0.853	**652840.919**	0.709	0.820	0.631	0.687	0.634	0.639
Spine 25	0.434	**0.062**	0.385	**0.160**	0.539	0.671	0.541	0.606
Spine 26	0.419	**0.063**	0.370	**0.198**	0.332	0.480	0.401	0.362
Spine 27	0.653	**0.079**	0.725	**0.308**	0.613	0.807	0.634	0.599
Spine 28	0.431	**0.064**	0.560	**0.278**	0.433	0.645	0.535	0.484
Spine 29	0.572	**0.029**	0.582	**0.276**	0.570	0.628	0.568	0.585
Spine 30	0.537	**0.081**	0.584	**0.315**	0.465	0.601	0.486	0.541
Spine 31	0.448	**0.036**	0.474	**0.232**	0.459	0.581	0.443	0.476
Spine 32	0.373	**0.041**	0.535	**0.363**	0.520	0.630	0.276	0.495
Spine 33	0.451	**0.072**	0.501	**0.337**	0.555	0.656	0.415	0.433
Spine 34	0.498	**0.062**	0.486	**0.165**	0.494	0.540	0.431	0.396
Average	0.692		0.679		0.702	0.745	0.687	0.700

Table 1. Quantitative results on 34 dendritic spines. Left: ***Experiment 1*** Right: ***Experiment 2***. Note that, spines between Spine 1 - Spine 24 are mushroom and between Spine 25 - Spine 34 are stubby.

proposed method that uses appearance feature priors produces very similar average Dice scores with the method in [9]. However, [9] gives wrong class decisions on 7 spines. Some visual segmentation results obtained in ***Experiment 2*** can be seen in Figure 2.

5. CONCLUSION

We have proposed a segmentation method that exploits joint shape and feature priors. Our method defines the prior shape probability as the joint probability of shapes and discriminative shape features and minimizes the resulting energy functional with level sets and gradient descent. We provide experimental results on dendritic spine segmentation in 2-photon microscopy images which presents a multimodal and complex shape density estimation problem. Experimental results demonstrate that the proposed algorithm achieves better segmentations than both Kim et al. [6] and Erdil et al. [9].

One possible future direction is to apply the proposed method to different data sets. Especially, performance of the proposed method on segmentation of 3D objects would be worth exploring. One might also consider building a similar approach on a different shape representation than level sets, e.g Disjunctive Normal Shape Models [15, 16]. Our approach can also be modified slightly and be used as a joint segmentation and classification approach. To this end, classes (perhaps corresponding to modes in the shape density) may be inferred during the segmentation phase and this probabilistic inference may then be used to update the weights of the training samples to drive the segmentation.

6. REFERENCES

[1] Masanori Matsuzaki, Naoki Honkura, Graham CR Ellis-Davies, and Haruo Kasai, "Structural basis of long-term potentiation in single dendritic spines," *Nature*, vol. 429, no. 6993, pp. 761–766, 2004.

[2] Arvind Govindarajan, Inbal Israely, Shu-Ying Huang, and Susumu Tonegawa, "The dendritic branch is the preferred integrative unit for protein synthesis-dependent ltp," *Neuron*, vol. 69, no. 1, pp. 132–146, 2011.

[3] Kristen M Harris, "Structure, development, and plasticity of dendritic spines," *Current opinion in neurobiology*, vol. 9, no. 3, pp. 343–348, 1999.

[4] Jan Tønnesen, Gergely Katona, Balázs Rózsa, and U Valentin Nägerl, "Spine neck plasticity regulates compartmentalization of synapses," *Nature neuroscience*, vol. 17, no. 5, pp. 678–685, 2014.

[5] Andy Tsai, Anthony Yezzi Jr, William Wells, Clare Tempany, Dewey Tucker, Ayres Fan, W Eric Grimson, and Alan Willsky, "A shape-based approach to the segmentation of medical imagery using level sets," *Medical Imaging, IEEE Transactions on*, vol. 22, no. 2, pp. 137–154, 2003.

[6] Junmo Kim, Müjdat Çetin, and Alan S Willsky, "Nonparametric shape priors for active contour-based image segmentation," *Signal Processing*, vol. 87, no. 12, pp. 3021–3044, 2007.

[7] Daniel Cremers, Stanley J Osher, and Stefano Soatto, "Kernel density estimation and intrinsic alignment for shape priors in level set segmentation," *International Journal of Computer Vision*, vol. 69, no. 3, pp. 335–351, 2006.

[8] Timothy F Cootes, Gareth J Edwards, and Christopher J Taylor, "Active appearance models," *IEEE Transactions on Pattern Analysis & Machine Intelligence*, , no. 6, pp. 681–685, 2001.

[9] Ertunc Erdil, Ali O. Argunsah, Tolga Tasdizen, Devrim Unay, and Mujdat Cetin, "A joint classification and segmentation approach for dendritic spine segmentation in 2-photon microscopy images," in *Biomedical Imaging (ISBI), 2015 IEEE 12th International Symposium on*, April 2015, pp. 797–800.

[10] Tony F Chan and Luminita Vese, "Active contours without edges," *Image processing, IEEE transactions on*, vol. 10, no. 2, pp. 266–277, 2001.

[11] David G Lowe, "Object recognition from local scale-invariant features," in *Computer vision, 1999. The proceedings of the seventh IEEE international conference on*. Ieee, 1999, vol. 2, pp. 1150–1157.

[12] David Mumford and Jayant Shah, "Optimal approximations by piecewise smooth functions and associated variational problems," *Communications on pure and applied mathematics*, vol. 42, no. 5, pp. 577–685, 1989.

[13] Muhammad Usman Ghani, Sumeyra Demir Kanik, Ali Ozgur Argunsah, Tolga Tasdizen, Devrim Unay, and Mujdat Cetin, "Dendritic spine shape classification from two-photon microscopy images," in *Signal Processing and Communications Applications Conference (SIU), 2015 23th*. IEEE, 2015, pp. 939–942.

[14] Lee R Dice, "Measures of the amount of ecologic association between species," *Ecology*, vol. 26, no. 3, pp. 297–302, 1945.

[15] Nisha Ramesh, Fitsum Mesadi, Mujdat Cetin, and Tolga Tasdizen, "Disjunctive normal shape models," in *Biomedical Imaging (ISBI), 2015 IEEE 12th International Symposium on*. IEEE, 2015, pp. 1535–1539.

[16] Fitsum Mesadi, Mujdat Cetin, and Tolga Tasdizen, "Disjunctive normal shape and appearance priors with applications to image segmentation," in *Medical Image Computing and Computer-Assisted InterventionMICCAI 2015*, pp. 703–710. Springer, 2015.